GPS Solut (2014) 18:51–60
DOI 10.1007/s10291-012-0309-1

ORIGINAL ARTICLE

Improved precise point positioning in the presence of ionospheric scintillation

Xiaohong Zhang · Fei Guo · Peiyuan Zhou

Received: 4 August 2012 / Accepted: 31 December 2012 / Published online: 16 January 2013

Abstract Ionospheric disturbances can be detrimental to accuracy and reliability of GNSS positioning. We focus on how ionospheric scintillation induces significant degradation to Precise Point Positioning (PPP) and how to improve the performance of PPP during ionospheric scintillation periods. We briefly describe these problems and give the physical explanation of highly correlated phenomenon of degraded PPP estimates and occurrence of ionospheric scintillation. Three possible reasons can contribute to significant accuracy degradation in the presence of ionospheric scintillation: (a) unexpected loss of lock of tracked satellites which greatly reduces the available observations and considerably weakens the geometry, (b) abnormal blunders which are not properly mitigated by positioning programs, and (c) failure of cycle slip detection algorithms due to the high rate of total electronic content. The latter two reasons are confirmed as the major causes of sudden accuracy degradation by means of a comparative analysis. To reduce their adverse effect on positioning, an improved approach based on a robust iterative Kalman filter is adopted to enhance the PPP performance. Before the data enter the filter, the differential code biases are used for GNSS data quality checking. Any satellite whose $C1$–$P1$ and $P1$–$P2$ biases exceed 10 and 30 m, respectively, will be rejected. Both the Melbourne–Wubbena and geometry-free combination are used for cycle slip detection. But the thresholds are set more flexibly when ionospheric conditions become unusual. With these steps, most of the outliers and cycle slips can be effectively detected, and a first PPP estimation can be carried out. Furthermore, an iterative PPP estimator is utilized to mitigate the remaining gross errors and cycle slips which will be reflected in the posterior residuals. Further validation tests based on extensive experiments confirm our physical explanation and the new approach. The results show that the improved approach effectively avoids a large number of ambiguity resets which would otherwise be necessary. It reduces the number of re-parameterized phase ambiguities by approximately half, without scarifying the accuracy and reliability of the PPP solution.

Keywords Ionospheric scintillation · Precise point positioning · Cycle slip detection · Quality control

X. Zhang (✉) · F. Guo · P. Zhou
School of Geodesy and Geomatics, Wuhan University,
129 Luoyu Road, Wuhan 430079, China
e-mail: xhzhang@sgg.whu.edu.cn

Introduction

Irregularities in electron density cause inhomogeneities in the refractivity of the radio frequency (RF) signals when traveling through the ionosphere. Rapid fluctuations of the phase and amplitude of RF signals appear to cause ionospheric scintillation (Aaron and Basu 1994). Degradation of performance due to the presence of ionospheric scintillation is a major problem in satellite communications and radar astronomical observations, particularly around equatorial and auroral region (Skone 2001; Moreno et al. 2011). GNSS satellite–receiver links traveling through the atmosphere are also vulnerable to ionospheric scintillation. It disturbs GNSS signals in several ways, including degradation of accuracy and loss of signal tracking (Seo et al. 2007). Extensive research about the occurrence of scintillation and its adverse effects on the performance of GNSS receivers has been reported in recent years (Moore et al. 2002; Alfonsi et al. 2006; Seo et al. 2007; Chen et al. 2008; Silva et al. 2010; Moreno et al. 2011; Demyanov et al. 2012). Recent studies have shown that the tracking performance depends not only

on the magnitude of scintillation, but also on the type of receiver. The signal-tracking performance of a receiver may vary widely between different manufacturers, tracking technologies, and firmware versions (Skone et al. 2004). During periods of small-scale ionospheric scintillation, both the pseudorange and carrier phase measurements may experience abnormal losses of lock or large errors (Aquino et al. 2007). Such effects have a larger impact on the L2 tracking loops, leading to a significant impact on precise positioning applications which require formation of wide-lane and/or ionosphere-free observables (Skone et al. 2001).

From the perspective of GNSS positioning, it is beyond the scope of this study to examine the physical aspects of the ionospheric scintillations and receiver-tracking technology. We are instead concerned about a mathematical approach or strategy which could possibly be advantageous during periods of scintillation. Ideally, the satellite–receiver links most affected by scintillation should be isolated and deleted from the solution. However, this could be detrimental to the quality of the resulting satellite geometry. To get a good positioning performance in the presence of ionospheric scintillation, Aquino et al. (2009) presented an improved stochastic model for GPS relative positioning. Scintillation indices such as S4 and σ_{φ} (Van Dierendonck 2001) recorded by specially designed GPS receivers were used to calculate the code and carrier phase tracking error variance according to the models described by Conker et al. (2003). Although the experiments and results are encouraging, further research is necessary for practical future use since most geodetic GNSS receivers do not measure scintillation parameters. To reduce the effects of sudden changes in geometry observed during epochs of signal loss, Moreno et al. (2011) defined a weighting function depending on the geometric dilution of precision (GDOP) for PPP solution. Nevertheless, there is no significant improvement during a period of ionospheric scintillation. Large variations of several meters in altitude/latitude can still be observed. Similar phenomena occurred during data processing by an online program CSRS–PPP (Canadian Spatial Reference System–PPP, Natural Resources of Canada, http://www.geod.nrcan.gc.ca/products-produits/ppp_e.php), reaching errors of several meters to tens of meters for kinematic PPP. The reason why an ionospheric scintillation induces a significant degradation of PPP is not yet clear and how to deal with this problem is unsolved. We show the reason why ionospheric scintillation degrades PPP estimates, beyond what is explained in Moreno et al. (2011). Then, an effective approach to improve PPP performance in the presence of ionospheric scintillation will be proposed and validated.

Problems presented by Moreno

Moreno et al. (2011) investigated the relationship between large changes in the rate of vertical total electronic content (TEC) and positioning errors in single-epoch PPP. Data recorded on April 18–22, 2004 (DOY 109–112), at MALI International GNSS Service (IGS) station located at equatorial latitudes were of particular interest, because high TEC gradients were observed during these days. In contrast, data recorded on April 17, 2004 (DOY 108), at two other IGS stations (MAS1, PRE1) located at middle latitudes were also studied by Moreno since no significant TEC gradients were observed. Figure 1 shows the rate of vertical TEC (ROT) units of TECU/30 s and corresponding epoch-wise PPP errors in meters at MALI during 10:00–22:00 UT on DOY 108, 109, and 112 of 2004. As shown in the first two columns of Fig. 1, during a day (DOY 108) with small TEC variation, the errors in altitude present variation of less than 0.5 m. However, there is a significant increase in the error of the MALI altitude estimates from 17:00 to 22:00 UT on days 109 and 112 when the values of ROT are irregular and large. To confirm these results obtained with single-epoch PPP, the same data were reprocessed in kinematic mode with the online program CSRS–PPP, and the errors in altitude are shown in the third column of Fig. 1. Corroborating the results in the second column of Fig. 1, the solution from CSRS also experienced large variations on days 109 and 112 for the MALI station. These errors reached 2 m on day 109 at about 20:00 and were higher than 20 m on day 112.

An unexpected loss of lock of a tracked satellite that weakens the geometry considerably would be reflected in a sudden increase of the geometric dilution of precision (GDOP), which would give rise to degraded positioning accuracy. In order to reduce and smooth the effect of poor satellite geometry and sudden loss of lock on the PPP estimation, the dependence on satellite geometry has been mitigated by means of GDOP based weighting in Moreno's solution. However, this does not eliminate the significant increase of positioning error during the periods of ionospheric scintillation. Therefore, in the above situation, the abrupt changes in the satellite geometry can be discarded as possible cause of such errors. So Moreno et al. (2011) point out that the presence of large ROT observed at equatorial latitudes can induce a significant degradation of dual-frequency PPP estimations. But the actual cause behind this phenomenon and actions for improvement are not investigated in detail.

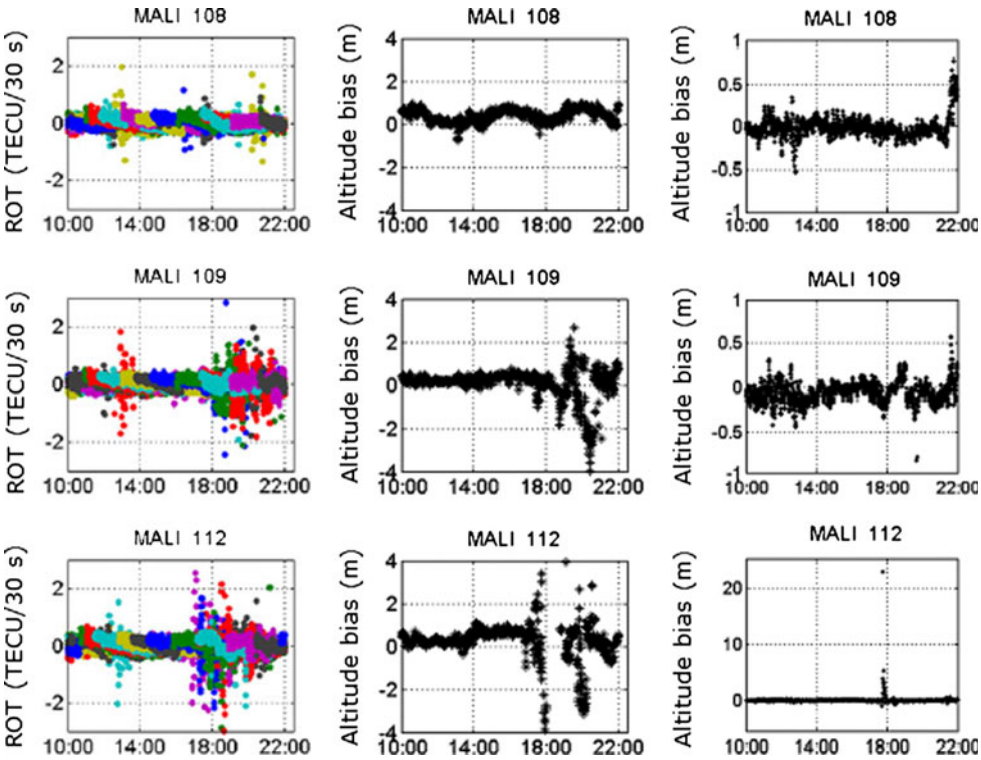

Fig. 1 ROT and PPP solutions of MALI on days 108, 109, and 112 of 2004 from Moreno. *Left column* shows the rate of vertical TEC obtained at MALI station for satellites over 15° elevation; middle column shows the estimated altitude biases obtained by Moreno; *right column* shows the estimated altitude biases obtained with CSRS–PPP. *Horizontal axis* shows time in UT

Influences of ionospheric scintillation on PPP

Three major potential reasons possibly contribute to the significant accuracy degradation in the presence of ionospheric scintillation: (a) unexpected loss of lock of tracked satellites which greatly reduces the number of available observations and weakens the geometry; (b) abnormal blunders which are not properly mitigated in PPP estimation; and (c) failure of cycle slips detection algorithms due to large ROT. Moreno et al. (2011) have investigated the first reason by comparing the number of satellite and GDOP values on days 108, 109, and 112. Nevertheless, there is no significant change in the number of satellites or signal geometry during the period from 17:00 to 22:00. This indicates that we can exclude the first potential reason as a cause of the abrupt variations in PPP solution. Therefore, in this work, we mainly focus on the latter two possibilities.

The effect of ionospheric scintillation on GNSS observables

The range measurements on a specific satellite-receiver link are widely described by the following equations (Gao et al. 2001):

$$C_1 = \rho + d\rho_{C1} + d_{\mathrm{sat}/C1} + d_{\mathrm{rcv}/C1} + S_{C1} + \varepsilon(C_1) \quad (1)$$

$$P_1 = \rho + d\rho_{P1} + d_{\mathrm{sat}/P1} + d_{\mathrm{rcv}/P1} + S_{P1} + \varepsilon(P_1) \quad (2)$$

$$P_2 = \rho + d\rho_{P2} + d_{\mathrm{sat}/P2} + d_{\mathrm{rcv}/P2} + S_{P2} + \varepsilon(P_2) \quad (3)$$

where ρ is the true geometric range between receiver and satellite, $d\rho$ is the range error that includes satellite orbit error, clock error, tropospheric delay and ionospheric delay, $d_{\mathrm{sat}/C1}$, $d_{\mathrm{rcv}/C1}$, $d_{\mathrm{sat}/P1}$, $d_{\mathrm{rcv}/P1}$, $d_{\mathrm{sat}/P2}$, and $d_{\mathrm{rcv}/P2}$ are the constant satellite and receiver biases on *C/A* code and *P* code pseudoranges, and S_{C1}, S_{P1}, and S_{P2} are satellite-independent but time-variant signals in *C*1, *P*1, and *P*2 pseudorange, respectively. The symbol $\varepsilon(\cdot)$ includes pseudorange noise and multipath effect.

In order to reveal the possible cause of accuracy degradation resulting from contaminated measurements, three observables are defined as,

$$dC_1P_1 = C_1 - P_1 = d_{\mathrm{sat}/C1-P1} + d_{\mathrm{rcv}/C1-P1} + S_{C1-P1} + \varepsilon \quad (4)$$

$$dP_1P_2 = P_1 - P_2 = d_{\mathrm{sat}/P1-P2} + d_{\mathrm{rcv}/P1-P2} + S_{P1-P2} + d_{\mathrm{iono}} + \varsigma \quad (5)$$

$$dL_1L_2 = \Delta(\lambda_1 L_1 - \lambda_2 L_2) = -\Delta d^j_{\mathrm{iono}} + \xi \quad (6)$$

where λ_1 and λ_2 are wavelength of L_1 and L_2, and $d_{\mathrm{sat}/C1-P1}$, $d_{\mathrm{rcv}/C1-P1}$, $d_{\mathrm{sat}/P1-P2}$, and $d_{\mathrm{rcv}/P1-P2}$ are differential constant satellite and receiver code biases between different code measurements, S_{C1-P1} and S_{P1-P2} are differential time-variant signals between different codes, Δ is the epoch difference operator, d_{iono} is the residual ionospheric delay, and ε, ς, and ξ are the combination of unknown residual errors, multipath effect and noise of each observable.

In Fig. 2, the time series of the three observables defined above for all satellites for days 108, 109, and 112 are presented for MALI. According to the left panels (MALI 108), it is clear that the time series of dC_1P_1 and dP_1P_2 behave as a combination of constant sequences and time-variant signals for each satellite as suggested by (4–5). Due to the ionospheric delay, dP_1P_2 is much larger than dC_1P_1, but the absolute value of both is no more than 20 m for almost all satellites during the whole period. The time series dL_1L_2 behaves like a noise sequence when large cycle slips are excluded; it varies within 0.1 m. When affected by several small cycle slips, the absolute value of dL_1L_2 can reach a few decimeters. As shown by the middle and right panels, we notice that the raw pseudoranges of a few satellites are greatly degraded during the periods of ionospheric scintillation (UT 18:00–22:00) on days 109 and 112. Sometimes, the discrepancies between $C1$, $P1$ and $P2$ could differ up to tens of kilometers. Moreover, the time series of dL_1L_2 does not behave like a noise sequence any longer due to the fast variation of ionospheric delay. The value of dL_1L_2 for most satellites is much larger than usual and shows a dispersive distribution. It should be noted that only those signals that travel through the disturbed ionosphere would present abnormal or unexpected observables. For a given epoch, only the pseudoranges of a few satellites are deteriorated while the observable of dL_1L_2 for most satellites are affected simultaneously.

Figures 1, 2 have corroborated a strong relationship between the deteriorated observables and accuracy degradation. The deteriorated measurements would lead to unexpected behavior of the positioning algorithms and software. Fortunately, most software is able to detect and excludes deteriorated code measurements which manifest as gross errors in the pre-processing stage. But the large residual ionospheric delay in observable dL_1L_2 decreases the reliability of cycle slip detection process, since the thresholds may be invalid during periods of ionospheric scintillation. Further validation of this phenomenon is presented in "Ionospheric scintillation effect on cycle slip detection" section.

Ionospheric scintillation effect on cycle slip detection

For the purpose of reliability, several methods are combined for cycle slip detection during the pre-processing stage. TurboEdit (Blewitt 1990) is a widely used algorithm for GNSS data editing. It covers the following two basic detection observables:

$$T_{\mathrm{GF}} = \Delta(\lambda_1 L_1 - \lambda_2 L_2) = (1-\alpha)\Delta I + \lambda_1 \Delta N_1 - \lambda_2 \Delta N_2 + \xi_{\mathrm{GF}} \quad (7)$$

$$T_{\mathrm{MW}} = \frac{1}{\lambda_{\mathrm{WL}}}(\Delta L_{\mathrm{WL}} - \Delta P_{\mathrm{NL}}) = \Delta N_1 - \Delta N_2 + \xi_{\mathrm{MW}} \quad (8)$$

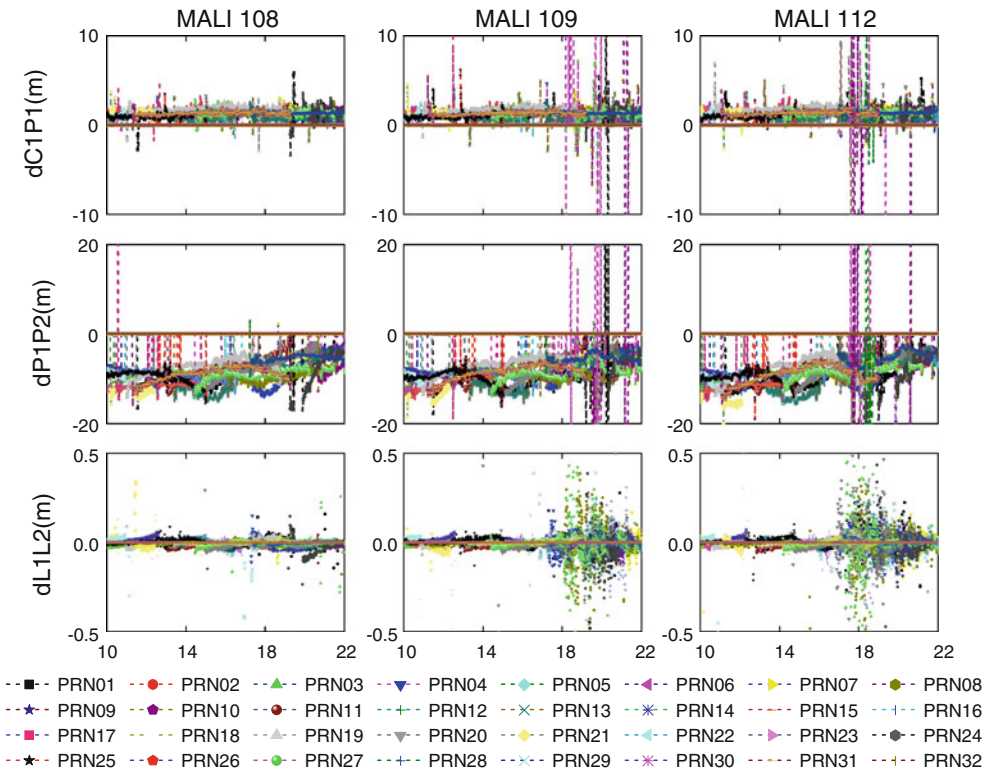

Fig. 2 Time series of dC_1P_1, dP_1P_2, dL_1L_2 on days 108 (*left*), 109 (*middle*), and 112 (*right*) at MALI station. The *horizontal axis* shows time in UT

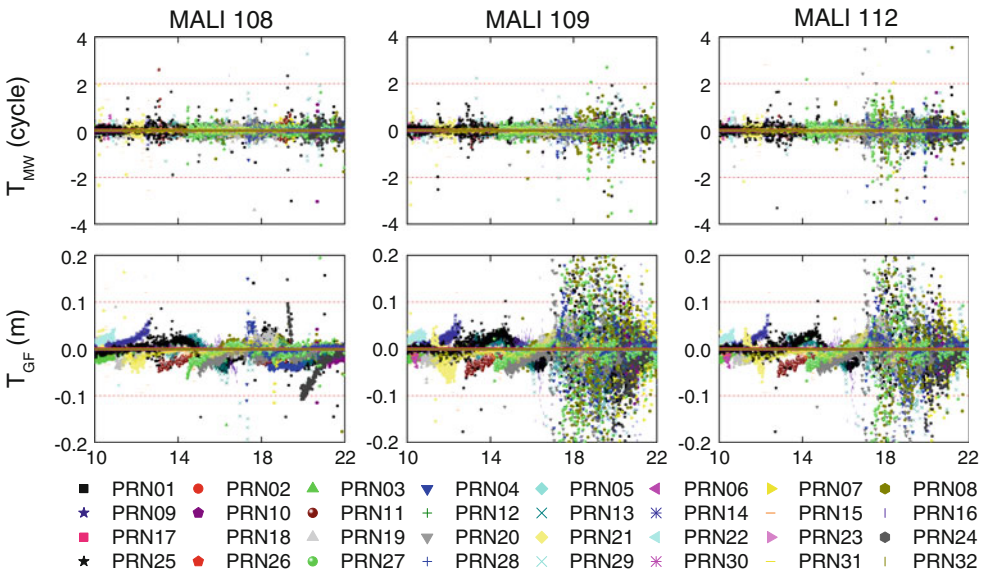

Fig. 3 Time series of T_{MW} and T_{GF} on days 108 (*left*), 109 (*middle*) and 112 (*right*) at MALI station. The *horizontal axis* shows time in UT

where T_{GF} and T_{MW} are, respectively, the geometry-free (GF) and Melbourne–Wubbena (MW) combination observables. L_{WL} is the wide-lane phase measurement, P_{NL} is the narrow-lane code measurement, N_1 and N_2 are the ambiguities of $L_1$and L_2,respectively, ξ is the combination of multipath and observation noise, and Δ is the epoch difference operator.

The T_{MW} function denotes the ionospheric-free delay and is insensitive to variations in non-dispersive delays, receiver-satellite relative motion, and tropospheric delay. However, T_{GF} is sensitive to ionospheric activity. The observable T_{GF} might not be modeled accurately if the residual ionospheric delay changes irregularly. The cycle slip detection algorithm when setting a strict threshold to decide whether a cycle slip happens appears to be overly conservative. Consequently, the default threshold value, for example, 0.05–0.15 m depending on sampling rate, may be invalid and must be reset to a more flexible value should ionospheric conditions become unusual. This may be a possible cause of accuracy degradation because ambiguities are frequently re-initialized unnecessarily in this case. To support this, the observables T_{MW} and T_{GF} of all available satellites under different ionosphere conditions were calculated and used separately for cycle slip detection. Figure 3 shows the time series of T_{MW} and T_{GF} during 10:00–22:00 UT on days 108, 109, and 112. The corresponding detection results, including the number of usable satellites N_{SV} and the number of detected cycle slips in N_{MW} and N_{GF}, are shown in Fig. 4. Since there is no unified threshold for all circumstances, the threshold value of T_{MW} and T_{GF} is commonly set to 1–2 cycles and 0.05–0.15 m, respectively.

Examining Fig. 3, we can find that both T_{MW} and T_{GF} are affected by ionospheric scintillation but with different degrees. During the disturbed ionosphere periods, most satellites keep a small and continuous T_{MW}. Only the T_{MW} of a few satellites are larger than usual because of the degraded code measurements. However, the value of T_{GF} changes rapidly and most of them are larger than 0.1 m. Fig. 4 shows that only 0–2 satellites were detected having cycle slips at the same time using either T_{MW} or T_{GF} observable during the quiet ionospheric conditions. Moreover, for any specific detection method, the detection results are quite similar at the same epoch (local time) from different days due to the repeatability of satellite orbits. However, the detection results are completely inconsistent with each other during

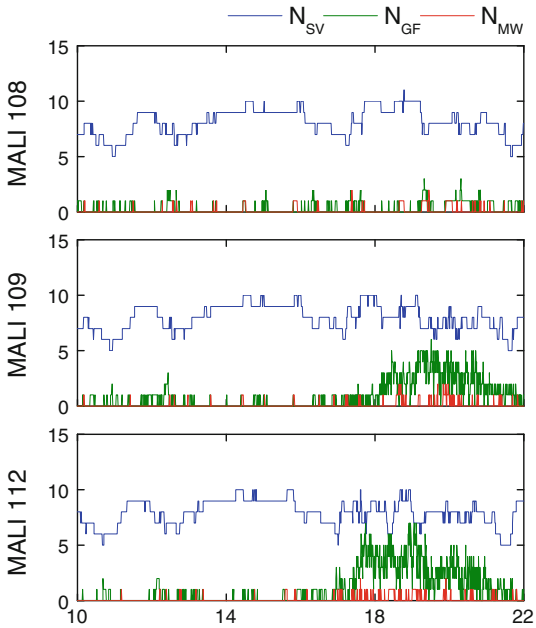

Fig. 4 The number of usable satellite N_{SV} and cycle slips in N_{MW} and N_{GF} on days 108 (*upper*), 109 (*middle*), and 112 (*lower*). The *horizontal axis* shows time in UT

18:00–22:00 UT on days 109 and 112. For a given epoch, the number of cycle slips detected by T_{MW} continues to be 0–2, but the number of satellites which are marked as affected by cycle slips reaches about 4–5 when using T_{GF} as a cycle slip indicator. Although the MW combination is insensitive to the extremely unlikely event that identical cycle slips occur on each frequency, the detection results from T_{MW} can be regarded as the true case with high confidence. Therefore, it can be concluded that T_{GF} is much more stringent than T_{MW}, but it is often spurious. This is reasonable when we acknowledge the fact that the GF combination is sensitive to ionospheric activity. The rapid variation of conditions in the ionosphere leads to an unexpectedly large residual ionospheric delay which far exceeds the default threshold set in the conventional algorithm.

It should be noted that the flagged cycle slips may not always be real cycle slips since optimal threshold values are critical but difficult to determine. In order to edit the GNSS data as cleanly as possible, relatively tight threshold values are usually adopted for preprocessing. Tight thresholds are more sensitive to cycle slips but sometimes may be overly conservative in determining whether a cycle slip has occurred. Clearly, frequent unnecessary ambiguity resets would weaken the positioning geometry and reliability of the parameter estimation. Further validations will be presented in "Performance testing" section.

An improved approach

To avoid accepting spurious cycle slips as true cycle slips, we propose a simple but robust method to deal with this problem and then improve the positioning accuracy in the presence of ionospheric scintillation. Figure 5 shows the flowchart of the improved approach in detail. First, we make a brief check of the differential code biases at a given epoch (i) so that any satellite (j) with blunders will be rejected. Furthermore, both MW and GF combinations as shown in (7–8) are used for cycle slip detection. Compared with the conventional method, relatively loose threshold values are chosen to reduce the adverse effect of ionospheric activity and avoid unnecessary ambiguity resets. With the first two steps, most of the gross errors can be successfully rejected and slips greater than 2 cycles will be marked and re-parameterized. Then, first PPP estimation will be conducted.

In Fig. 5, the constants K_1–K_4 are the thresholds of the observable dC_1P_1, dP_1P_2, $T_{MW,}$ and $T_{GF,}$ respectively. To obtain proper threshold values, large data sets recorded by different GPS receiver types have been collected to analyze the variation of the four observables. Since T_{MW} is less sensitive to ionospheric condition and can be refined by averaging algorithm, we mainly focus on the other three observables. A few typical examples are presented in Fig. 6 which shows the time series of dC_1P_1, dP_1P_2, dL_1L_2 on MALI, GLPS, and WUHN at day 110, 2004.

As illustrated in Figs. 2 and 6, the difference between coarse code (C) and precise code (P), that is, dC_1P_1, ranges from decimeters to a few meters on the same frequency. The code bias between different frequencies dP_1P_2 is about 2–3 times larger than dC_1P_1 and shows a significant time-varying signal. It should be noted that sometimes C_1 and P_1 may not be simultaneously available (e.g. C_1, P_2, $L_{1,}$ and L_2), and then, dC_1P_1 and dP_1P_2 cannot be used for

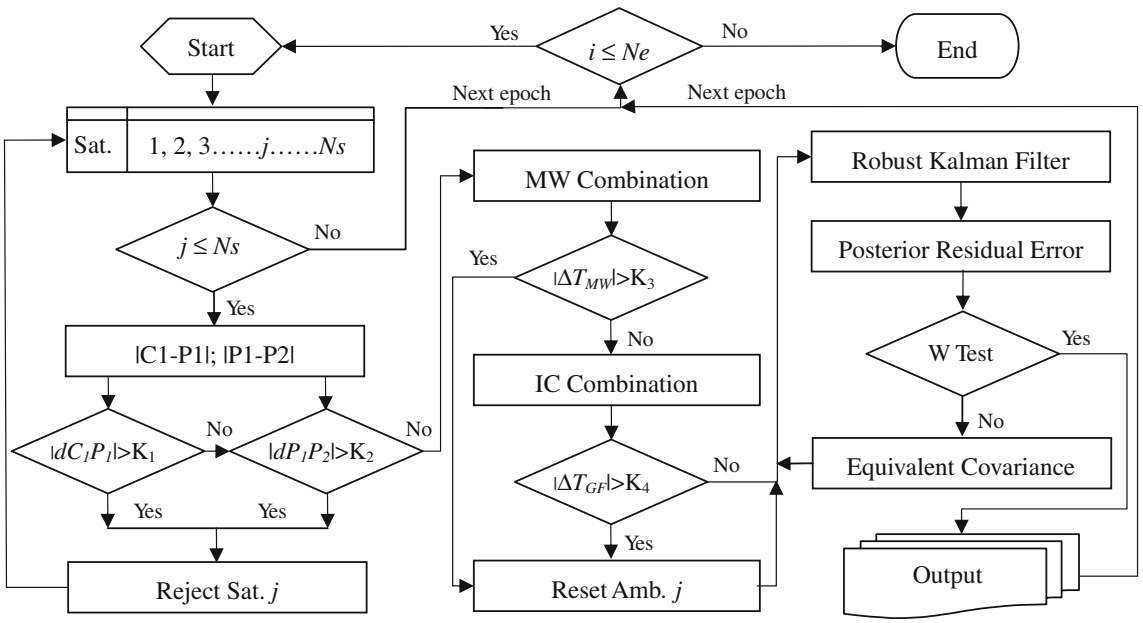

Fig. 5 Procedure of the improved approach

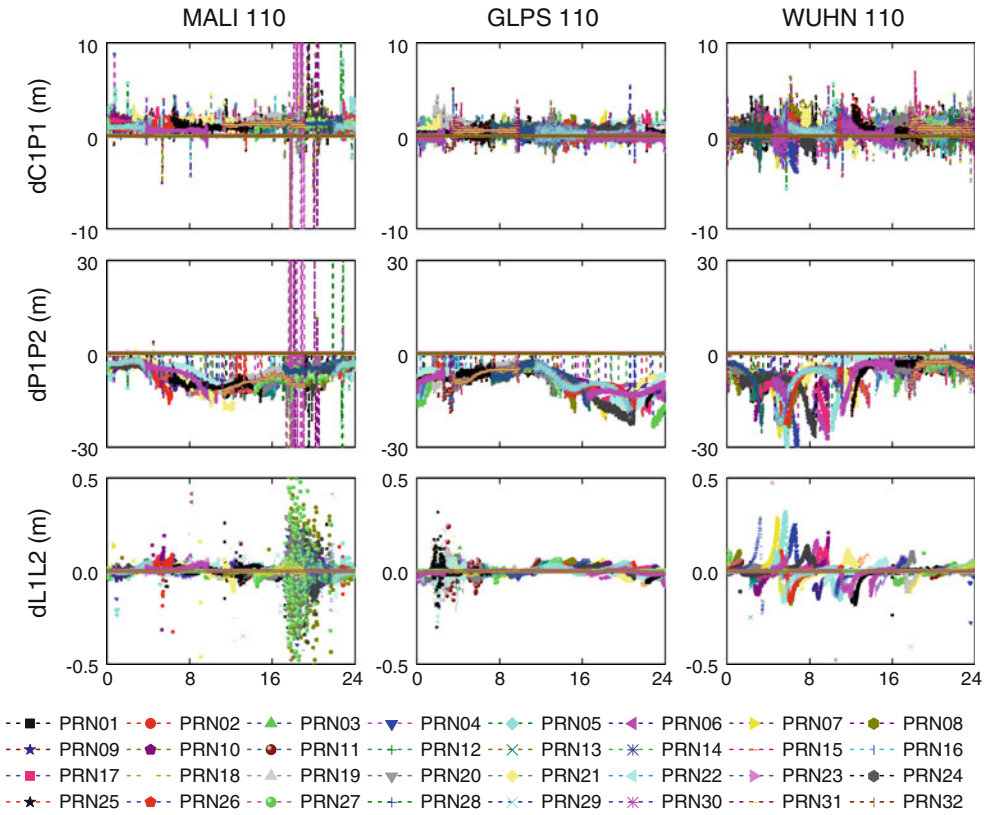

Fig. 6 Time series of dC_1P_1, dP_1P_2, dL_1L_2 at MALI (*left*), GLPS (*middle*), and WUHN (*right*) on day 110. The *horizontal axis* shows time in UT

pseudorange quality check. In this case, P_1 can be substituted by C_1 for computing dC_1P_2. With regard to dL_1L_2, it is only a few centimeters for most of the time when large cycle slips are excluded, but sometimes it reaches about 0.3–0.5 m due to the sudden ionospheric disturbance and multipath effect. Therefore, for the sake of simplicity and uniformity, the threshold values are given as follows:

$$\begin{cases} K_1 = 10 \text{ m}; \quad K_2 = 30 \text{ m} \\ K_3 = 2 \text{ cycle}; \quad K_4 = 0.5 \text{ m} \end{cases} \tag{9}$$

In the first PPP estimation, a few small cycle slips are possibly ignored since relatively loose threshold values were set for cycle slip detection. This would definitely have adverse effects on the subsequent positioning results. Fortunately, the remaining outliers and small cycle slips that have not been detected for the first runs will be reflected in the posterior residual errors. Therefore, further compensations could be made by introducing a weight function (Yang et al. 2001),

$$\bar{p}_j = \begin{cases} p_j & |\tilde{v}_j| \le h_0 \\ p_j \frac{h_0}{|\tilde{v}_j|} \left(\frac{h_1 - |\tilde{v}_j|}{h_1 - h_0} \right)^2 & h_0 < |\tilde{v}_j| \le h_1 \\ 0 & |\tilde{v}_j| > h_1 \end{cases} \tag{10}$$

where $\tilde{v}_j$ is the standardized residual of satellite j; p_j and $\bar{p}_j$ refer to the prior and posterior (or equivalent) weight; h_0 and h_1 are constants. Practical values for h_0 are 1.0–1.5 and 3.0–4.5 for h_1(Yang et al. 2001).

Obviously, the value $\bar{p}_j$ decreases as $\tilde{v}_j$ increases. The three-segment function adaptively decreases the contribution of remaining outliers and cycle slips in the following filtering. Once the covariance matrix of the observation equation is adapted, the stochastic mode of the state transition equation should be adjusted simultaneously so that the error of the predicted states such as predicted ambiguities will not influence the updated estimates. In this case, the remaining cycle slips will be compensated by means of ambiguity re-initialization.

Performance testing

In order to illustrate the performance of our approach, we used data sets recorded in static and kinematic modes, and in quiet and disturbed ionospheric situations. Since we are more concerned with the epoch-wise PPP solution during periods of ionospheric scintillation, only a few kinematic examples are shown in this section. For comparison, the

PPP software TriP developed at Wuhan University (Zhang and Andersen 2006) is used for a PPP solution with both the conventional and improved approaches. The conventional approach uses the TurboEdit algorithm with tight thresholds for GNSS data editing, while the improved approach sets looser thresholds but combines this with data snooping and robust estimation.

To validate our physical explanation as presented in "Influences of ionospheric scintillation on PPP" section, we first investigate the kinematic PPP performance using the same data as selected by Moreno et al. (2011). The corresponding positioning results including the estimated latitude (Lat), longitude (Lon), and altitude (Alt) were obtained, and the differences with respect to IGS05 position are presented in Fig. 7. In these plots, the blue curves show the positioning error of the conventional approach, and the red ones show the positioning error of the improved approach.

It can be observed here that the positioning error varies by less than 0.2 m in horizontal and 0.5 m in vertical direction for most of the time, particularly during day 108, which was a quiet day. This shows that without ionospheric disturbance, there is no significant discrepancy between the positioning accuracy of both the conventional and improved approach. However, large variations up to several meters can be observed on days 109 and 112 during the periods 17:00–22:00 UT when conventional approach was adopted for epoch-wise PPP solution, which is in agreement with the solutions of Moreno et al. (2011) and CSRS–PPP. The red curve shows that we can obtain smoothly running and accurate coordinate solutions even under the presence of ionospheric scintillation once the improved approach is introduced. Consequently, this supports our point of view for the accuracy degradation during the disturbed ionospheric conditions as given in "Influences of ionospheric scintillation on PPP" section.

Further validations have been performed for data from IGS stations NKLG (N 0.3°, E 9.6°) and GLPS (N −0.7°, E −90.3°), which are both located in equatorial regions and therefore under the influence of ionospheric scintillation. Figure 8 shows the number of re-parameterized phase

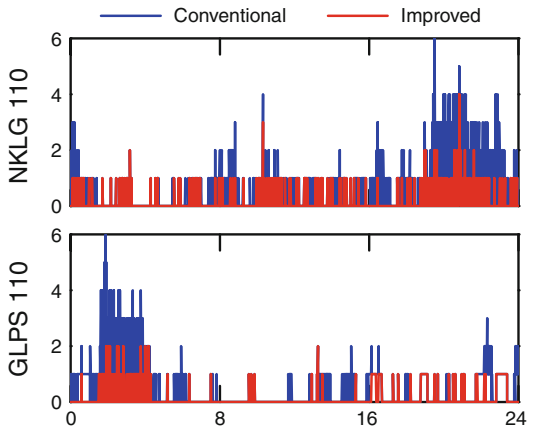

Fig. 8 Number of re-parameterized phase ambiguities of NKLG (*upper*) and GLPS (*lower*) on day 110 of 2004. The *blue curve* shows the results of conventional approach, and the *red* one shows the corresponding results of improved approach. The *horizontal axis* shows time in UT

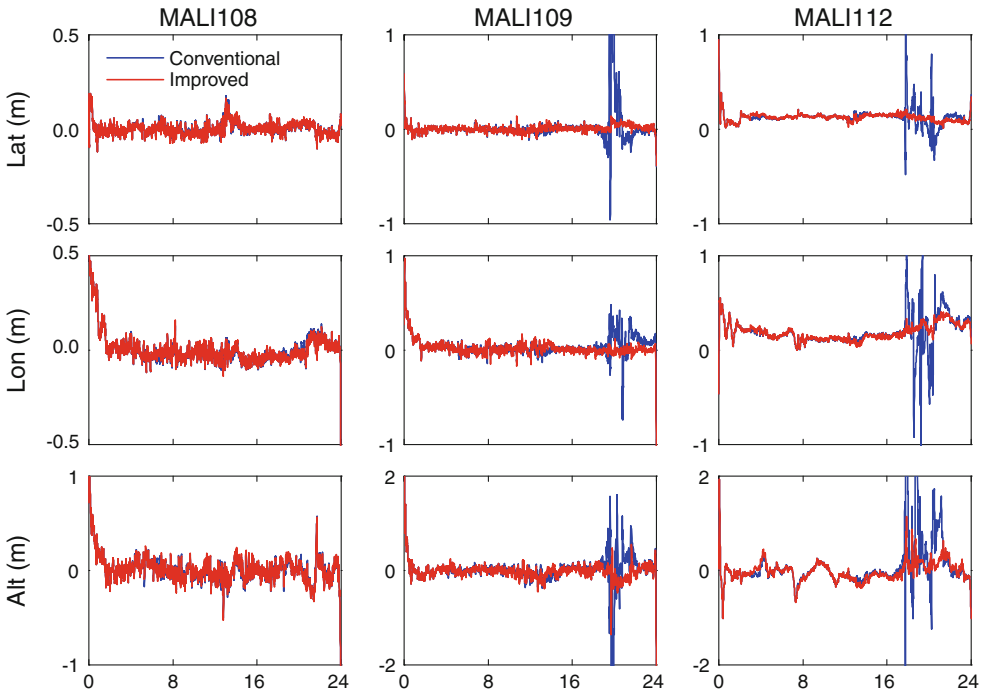

Fig. 7 Estimated coordinates on days 108 (*left*), 109 (*middle*), and 112 (*right*) of 2004 at MALI station. The *blue curve* shows the performance of conventional approach, and the *red* one shows the PPP performance of improved approach. The *horizontal axis* shows time in UT

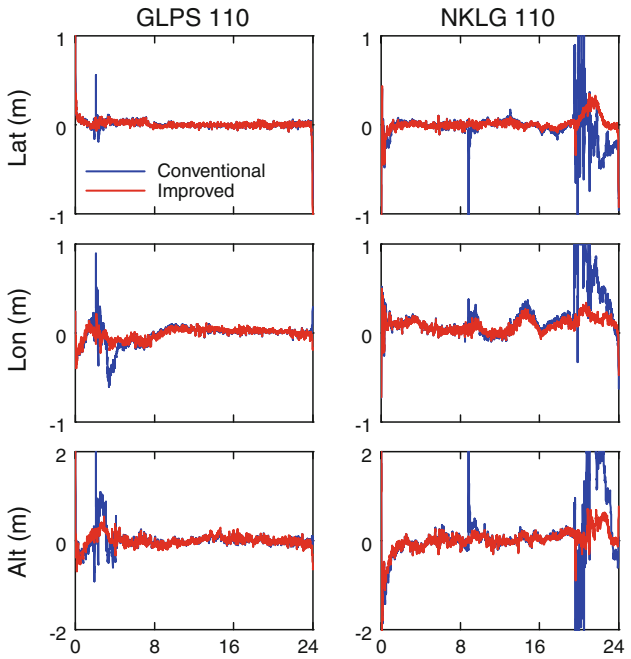

Fig. 9 Estimated coordinates of GLPS (*left*) and NKLG (*right*) station on day 110 of 2004. The *blue curve* shows the performance of conventional approach, and the *red* one shows the performance of improved approach. The *horizontal axis* shows time in UT

ambiguities of these two stations on day 110 of 2004, and Fig. 9 shows the consequent positioning accuracy based on the conventional and improved PPP algorithm. Similarly, the blue and red curves correspond to the results of conventional and improved approach, respectively.

As mentioned in "Influences of ionospheric scintillation on PPP" section, the conventional approach is extremely sensitive to the ionospheric anomalies. Sometimes, satellites will be erroneously marked as having cycle slips, leading to an increase in the number of re-parameterized phase ambiguities. Due to this increase in the number of ambiguity parameters as shown in Fig. 8, the PPP performance decreases significantly during the periods from 19:00 to 23:00 UT at NKLG and 02:00–04:00 UT at GLPS. Compared with the conventional approach, the improved algorithm effectively avoids a large number of unnecessary ambiguity resets by means of loosening the thresholds. It reduces by half the number of re-parameterized phase ambiguities, without scarifying the accuracy and reliability of the PPP solution. This is reasonable taking into account that a robust Kalman filter combined with data snooping is applied for further quality control during the processing stage. With the improved approach, the positioning accuracy reaches about 0.1–0.2 m in the horizontal and 0.2–0.3 m in the vertical direction during periods of ionospheric scintillation after a short initialization period.

Discussion and conclusions

Performance degradation due to ionospheric scintillations is a major problem in GNSS applications. Ionospheric scintillation disturbs GNSS positioning in a number of ways, including degradation of accuracy through range errors and the loss of signal tracking. Concentrating on the problem of why a large ROT is accompanied by positioning degradation and how to improve the PPP performance, which were not fully explained and investigated by Moreno et al. (2011), we discussed possible causes of accuracy degradation and put forward an improved approach to enhance the accuracy and reliability of PPP.

To eliminate large positioning errors during ionospheric disturbances, an improved approach has been proposed, and numerical experiments have been performed for validation. The results show that the improved approach is able to avoid unnecessary rejection or re-initialization, it reduces by half the number of re-parameterized phase ambiguities without scarifying the accuracy and reliability of the PPP solution. This method prevents the sudden variations in estimated position that are common in periods of ionospheric scintillation and maintains the position estimate with an accuracy of about 0.1–0.2 m in horizontal and 0.2–0.3 m in vertical, which represents a large improvement over conventional approaches. However, a problem worthy to be pointed out is that, even though the improved approach may effectively distinguish true cycle slips from spurious ones in the presence of ionospheric scintillation, it is unable to improve the PPP performance when real cycle slips are present.

Acknowledgments The authors gratefully acknowledge IGS and CODE community for providing global GNSS data and products. We also appreciate two anonymous reviewers and the editor in chief for their valuable comments and improvements to this manuscript. This study was supported by the Funds for Innovative Research Group of the National Natural Science Foundation of China (Grant No. 41021061) and National Natural Science Foundation of China (Grant No. 41074024 and No. 41204030).

References

Aaron J, Basu S (1994) Ionospheric amplitude and phase fluctuations at the GPS frequencies. In: Proceedings of the ION GPS-94, The Institute of Navigation, Salt Lake City, pp 1569–1578

Alfonsi, L, De Franceschi, G, Romano, V, Aquino, M and Dodson, A (2006) Positioning errors during the space weather event of October 2003. Location, ISSN 0973-4627, 1, issue 5

Aquino M, Andreotti M, Dodson A, Strangeways H (2007) On the use of ionospheric scintillation indices as input to receiver tracking models. J Adv Space Res 40(3):426–435

Aquino M, Monico J, Dodson A, Marques M, Franceschi G, Alfonsi L, Romano V, Andreotti M (2009) Improving the GNSS positioning stochastic model in the presence of ionospheric scintillation. J Geodesy 83(10):953–966. doi:10.1007/s00190-009-0313-6

Blewitt G (1990) An automated editing algorithm for GPS data. Geophys Res Lett 17(3):199–202
Chen W, Gao S, Hu CW, Chen YQ, Ding XL (2008) Effects of ionospheric disturbances on GPS observation in low latitude area. GPS Solut 12(1):33–41. doi:10.1007/s10291-007-0062-z
Conker RS, El-Arini MB, Hegarty CJ, Hsiao T (2003) Modeling the effects of ionospheric scintillation on GPS/satellite-based augmentation system availability. Radio Sci 38(1):1001. doi:10.1029/2000RS002604
Demyanov V, Yasyukevich Y, Ishin A, Astafyeva E (2012) Ionospheric super-bubble effects on the GPS positioning relative to the orientation of signal path and geomagnetic field direction. GPS Solut 16(2):181–189. doi:10.1007/s10291-011-0217-9
Gao Y, Lahaye F, Heroux P, Liao X, Beck N, Olynik M (2001) Modeling and estimation of C1–P1 bias in GPS receivers. J Geodesy 74(9):621–626. doi:10.1007/s001900000117
Moore T, Aquino M, Waugh S, Dodson A, Hill C (2002) Evaluation of the EGNOS ionospheric correction model under scintillation in Northern Europe. In: Proceedings of the ION GPS, The Institute of Navigation, Portland, Oregon, USA, pp 1297–1306
Moreno B, Radicella S, de Lacy MC, Herraiz M, Rodriguez-Caderot G (2011) On the effects of the ionospheric disturbances on precise point positioning at equatorial latitudes. GPS Solut 15(4):381–390. doi:10.1007/s10291-010-0197-1
Seo J, Walter T, Marks E. Chiou TY, Enge P (2007) Ionospheric Scintillation Effects on GPS receivers during solar minimum and maximum. In: Proceedings of the International Beacon Satellite Symposium 2007, 11–15 June 2007, Boston, MA
Silva HA, Camargo PO, Monico JFG, Aquino M, Marques HA et al (2010) stochastic modelling considering ionospheric scintillation effects on GNSS relative and point positioning. Adv Space Res 45(9):1113–1121
Skone SH (2001) The impact of magnetic storms on GPS receiver performance. J Geod 75(6):457–468
Skone S, El-Gizawy M, and Shrestha S (2001) Limitations in GPS positioning accuracies and receiver tracking performance during solar maximum. In: Proceedings of the international symposium on kinematic systems in geodesy, geomatics, and navigation. Banff, Alberta, June 5–8, pp 129–143
Skone S, Yousuf R, Coster A (2004) Performance evaluation of the wide area augmentation system for ionospheric storm events. J Glob Position Syst 3(1–2):251–258
Van Dierendonck AJ (2001) Measuring ionospheric scintillation effects from GPS signals. In: Proceedings of 57th annual meeting of the Institute of Navigation, Albuquerque, New Mexico, USA, pp 391–396
Yang Y, He H, Xu G (2001) A new adaptively robust filtering for kinematic geodetic positioning. J Geodesy 75(2):109–116
Zhang XH, Andersen OB (2006) Surface ice flow velocity and tide retrieval of the Amery ice shelf using precise point positioning. J Geod 80(4):171–176

Author Biographies

Dr. Xiaohong Zhang is currently a professor at the Wuhan University. He obtained his B.Sc., Master, and Ph.D. degrees with distinction in Geodesy and Engineering Surveying at the School of Geodesy and Geomatics in Wuhan University in 1997, 1999, and 2002. His main research interests include Precise Point Positioning (PPP) and GNSS/INS.

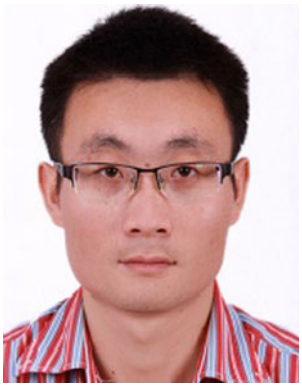

Fei Guo is currently a Ph.D. candidate at school of Geodesy and Geomatics, Wuhan University, China. He obtained his B.Sc. and M.Sc degrees in 2007 and 2009, respectively. His current research focuses mainly involve GNSS precise point positioning and quality control technology, etc.

Peiyuan Zhou is a Master student at the School of Geodesy and Geomatics, Wuhan University, China. He obtained his B.Sc. degrees in 2012. His main research focuses on the effect of atmosphere on precise GNSS positioning and high-precision GNSS applications.